Available online at www.sciencedirect.com
SCIENCE DIRECT
International Journal of Heat and Mass Transfer 49 (2006) 198–206
International Journal of HEAT and MASS TRANSFER
www.elsevier.com/locate/ijhmt

Flame dynamics in thin semi-closed tubes at different heat loss conditions

K.V. Dobrego *, I.M. Kozlov, V.V. Vasiliev

Heat and Mass Transfer Institute, National Academy of Sciences of Belarus, P. Brovki Street 15, Minsk 220072, Belarus

Received 15 July 2005
Available online 21 November 2005

Abstract

The results of detailed 2D numerical simulation of non-steady methane–air flame propagation in semi-closed tubes after ignition near the closed end are presented. Flame dynamics dependence on the tubes width for adiabatic and non-adiabatic walls is obtained. It is shown that main mechanism of front acceleration is flame surface perturbation due to hydrodynamic drag near the walls, which grows due to gas thermal expansion and flow acceleration. The mechanism of vortex formation in vicinity of the front bow point is demonstrated. The vortex is generated at the flame front velocities of the order of $S_l \sim 20$ m/s and may become precursor for flow turbulization at later instants.

The new theoretically possible regime of gas combustion in adiabatic conditions in narrow capillary is found. It is characterized by relatively low propagation velocity and incomplete combustion.

1. Introduction

Propagation of normal flames in ducts [1,2], flames quenching in narrow channels, slits, porous media [3] were under investigation starting from the first half of 20th century. More detailed study of flame shape and structure was performed with development of experimental and numerical simulation technique [4,5]. Fluid motion and flame shape was examined for lean limit methane flames in 51 mm diameter tube by Jarosinski et al. [6]. The dynamics and formation of curved "tulip" flame were experimentally and numerically examined in closed rectangular vessel by Dunn-Rankin et al. [7] neglecting low scale hydrodynamic movements and vorticity. Lee and Tien [8] present a study of flame quenching and flame flashback as a function of incoming velocity profiles, wall velocity gradients and tube radius.

Schelkin one of the first gave explanation of flames acceleration in the tubes [9]. According to Schelkin flame acceleration does not depend on temperature and pressure variation caused by pressure waves and controlled by flow gas dynamics, turbulization caused by flow drag on the wall. The questions of flames acceleration in tubes were treated theoretically and experimentally in further works by Soloukhin, Oppenheim and others [10,11]. Despite of profound physical analysis, the models describing flame acceleration mostly has a qualitative character. Rapid growth of computational powers in the last years gave one new possibilities of numerical simulation of flames propagation in tubes. Theoretical and numerical studies have been performed of a Poiseuille

* Corresponding author. Tel.: +375 17 2842021; fax: +375 17 2842212.
E-mail address: kdob@itmo.by (K.V. Dobrego).

0017-9310/$ - see front matter © 2005 Elsevier Ltd. All rights reserved.
doi:10.1016/j.ijheatmasstransfer.2005.08.020

Nomenclature

A_0	tube cross-section area or non-perturbed flame front surface area
A_f	flame front surface area
a_{ij}	polynomial coefficients in CHEMKIN database
c	heat capacity
D	gas diffusivity
d_0	tube diameter
d_{cr}	critical diameter of non-adiabatic tube
d_{cr1}	critical diameter of adiabatic tube
H	gas mixture enthalpy
h_i	enthalpy of ith gas component
k	preexponent
L	tube length
l_f	flame front width
$l_{f,w}$	distance between front leader point and tube wall
M	molar mass of gas mixture
M_i	molar mass of ith gas component
$\dot{m}$	combustion mass velocity
N	number of chemical components
$\mathbf{n}$	normal vector
p	pressure
p_0	pressure at exit cross-section
R	universal gas constant
r	radial coordinate
S_l	normal laminar flame velocity
S_f	flame velocity relative to walls
$S_{f,max}$	maximum flame velocity
s_i	stoichiometric coefficient
T	temperature
T_0	initial gas temperature
T_{ad}	adiabatic temperature
T_w	walls temperature
t	time
$\mathbf{u}$	gas mass velocity
v_i	ith component of gas mass velocity
v_z	longitudinal component of gas mass velocity
v_r	radial component
Δx	spatial grid step
Y_i	mass fraction of ith gas component
Y_{CH_4}	methane mass fraction
z	coordinate along the tube axis
$z_{f,max}$	coordinate of the front bow point

Greek symbols

α	heat exchange coefficient $\delta_{ik} = \begin{cases} 1, & i = k \\ 0, & i \neq k \end{cases}$
λ	thermal conductivity coefficient
μ	viscosity factor
ρ	gas density
ρ_b	combustion products density
$\dot{\rho}_i$	ith gas component chemical generation rate
σ'	viscous tensions tensor
ξ_{CH_4}	dimensionless methane concentration

flow with a flame in a tube [12,13]. These did not solve the full Navier–Stokes equations (assume constant density, for example) but looked at the effects of flame propagation in adiabatic and non-adiabatic walls. In recent works [14,15] the evolution of flames in flow that produces a shock and boundary layers ahead of the flame has been studied. These works, however, applies to different physical conditions, considering relatively large channels, or emphasis on events occurring much later in the evolution of the flow than those considered in this paper. In the work by Ott [16] an acetylene–air low pressure (0.132 atm) flame acceleration in narrow semi-closed tube was simulated by solving Navier–Stokes equations for compressible gas. Flame accelerating is found to be the only regime of combustion in adiabatic conditions. In conditions of constant temperature walls an oscillation motion of front was obtained. The influence of the boundary layer was discussed, although flame dynamics dependence on the tube width, and questions of turbulence generation were not touched.

In this work the results of the 2D numerical simulation of non-steady flame propagation in thin semi-closed tubes after ignition near the closed end are presented. We put attention to peculiarities of hydrodynamics of the process, particularly, associated with viscous tension at the walls, flame acceleration dependence on the tube width and formation of vortices in the flame. The problem was solved on high resolution uniform mesh. The gross model of chemical kinetics for methane–air combustion was accepted. It is shown that acceleration rate increases with the tube diameter decrease until critical diameter is reached. For adiabatic walls acceleration rate is higher, it grows with tube diameter decrease until much smaller critical diameter. In the "sub critical" tube a specific steady-state combustion regime takes place, characterized with relatively small velocity and incomplete fuel burn out.

2. Problem statement

Non-steady gas dynamics of chemically reacting gas can be described by set of equations: continuity, Navier–Stokes, mass conservation for gas components and energy conservation.

$$\frac{d\rho}{dt} = -\rho\nabla\mathbf{u}, \tag{1}$$

$$\rho\frac{d\mathbf{u}}{dt} = -\nabla p + \nabla\boldsymbol{\sigma}', \tag{2}$$

$$\rho\frac{dY_i}{dt} = \dot{\rho}_i + \nabla\cdot(\rho D\nabla Y_i), \quad i = \overline{1,N}. \tag{3}$$

Here $\dot{\rho}_i$—ith component mass generating rate due to chemical reaction (8), $\sum_i \dot{\rho}_i = 0$; D—diffusion coefficient, $\boldsymbol{\sigma}'$—viscous tensions tensor with components: $(\boldsymbol{\sigma}')_{ik} = \mu(\frac{\partial v_i}{\partial x_k} + \frac{\partial v_k}{\partial x_i} - \frac{2}{3}\delta_{ik}\frac{\partial v_l}{\partial x_l})$. Energy conservation equation is written in form of enthalpy conservation with regard to diffusion and heat conductivity processes

$$\rho\frac{dH}{dt} = \nabla\cdot\left(\rho\sum_i h_i D\nabla Y_i + \lambda\nabla T\right), \tag{4}$$

where h_i—mass enthalpy of ith gaseous component, λ—heat conductivity coefficient. Speed of sound is assumed to be infinitely high.

State of gas in arbitrary point is defined by pressure p_0, temperature T, gas velocity $\mathbf{u}$, gas components mass fractions Y_i together with gas state equations $\rho = \frac{p_0 M}{RT}$ and $H(T, Y_1, \ldots, Y_N) = \sum_i^N Y_i h_i(T)$, where $h_i(T)$ is expressed via polynomials according to CHEMKIN thermodynamics database [17]

$$\frac{M_i h_i}{RT} = \sum_{j=1}^{5}\frac{a_{ji}}{j}T^{j-1} + \frac{a_{6i}}{T}.$$

Mean molar mass of the gas M is expressed via component concentrations and mass $\frac{1}{M} = \sum_i \frac{Y_i}{M_i}$.

At the initial time instant gas has temperature $T_0 = 300$ K. Combustion ignition is simulated by setting temperature step function near the closed end of the tube (floor temperature—T_0, top temperature—T_{ad}) so that pressure remains constant and equal to p_0.

As far as velocity field is determined by pressure field (according to simulation method) boundary conditions applied to the pressure filed as follows. Impermeability and non-slip condition at the tube's walls:

$$\begin{cases} (\mathbf{n}\cdot\nabla)p = 0; \\ v_z|_{r=R} = 0; \\ v_r|_{z=0} = 0; \end{cases} \tag{5}$$

constant pressure condition at the open end cross-section:

$$p = p_0 \quad \text{at } (z = L). \tag{6}$$

Conditions of impermeability are implied to gas components concentrations at tube's walls

$$(\mathbf{n}\cdot\nabla)Y_i = 0. \tag{7}$$

Heat losses are taken into account by the boundary conditions [18]

$$\lambda\left.\frac{\partial T}{\partial r}\right|_{r=R} = \alpha(T|_{r=R} - T_w),$$

where T_w—walls temperature, $\alpha = 100\,\frac{W}{K\ m^2}$.

Reasonably simplified models of diffusion, heat conductivity and viscosity were used. Air heat conduction coefficient and viscosity were used in calculations. The following approximations with characteristic accuracy 5% in all temperature range were utilized: $\lambda = 1.4\times10^{-2} + 4.8\times10^{-5}T, \frac{W}{m\ K}$; $\mu = 4.4\times10^{-7}T^{0.65}, \frac{kg}{m\ s}$,

$$D = 1.13\times10^{-4}\frac{T^{1.7}}{p_0}, \ \frac{m^2}{s}.$$

Gross chemistry model of first order by methane was used as a model of chemical kinetics of combustion [19]

$$CH_4 + 2O_2 \rightarrow 2H_2O + CO_2,$$

$$\dot{\rho}_i = -\rho s_i k\exp(-E/T)Y_{CH_4}, \tag{8}$$

where s_i—stoichiometric coefficient for ith component, k—preexponent, $k = 2.6\times10^8\ s^{-1}$, Y_{CH_4}—methane mass fraction, $E = 15{,}640$ K.

Adiabatic combustion temperature for stoichiometric methane–air mixture was $T_{ad} = 2256$ K, normal laminar flame velocity was $S_l = 0.34$ m/s for this chemical kinetics model. Flame front width l_f, calculated by formula $(\lambda/c\rho)/S_l$ at the temperature of the chemical heat release ignition was $l_f = 0.3$ mm. This value was used as characteristic length scale of the problem.

2DBurner software application package was used for simulation [20]. Analogue of the MAC method generalized for calculating of slow axis-symmetric flows of a compressible gas taking into consideration thermal conductivity, mass diffusion and viscosity force was used for prediction of the gas motion. A similar method for gas free convection flows is delineated in [21]. Implicit time integration method based on Newton iterative one was used for solving kinetic equations system (3) simultaneously with energy equation (4).

Combustion gas dynamics in semi-closed tubes was simulated in the case of ignition near the closed end of the tube. Stoichiometric methane–air mixture was taken as a combustible. The length of the simulated tube was 4 cm and diameter of the channel varied in the range from 0.7 to 5 mm. The space step of the mesh was $\Delta x = 0.01$ or 0.02 mm which guaranteed spatial resolution of concentration fields, temperature front and boundary layers. Combustion ignition was simulated with temperature step at the 0.5 mm length domain near the closed end of the tube at the initial instant. The gas composition and temperature of the preheated domain corresponded to equilibrium at adiabatic combustion temperature T_{ad}. Combustion front position was defined as a line of the 0.5 level of the initial concentration of methane, $\xi_{CH_4} = 0.5$. The velocity of the bow point of the front relatively to the walls $S_{f,max}$ was considered

as main characteristic of the flame front propagation dynamics.

3. Simulation results

According to calculations, flame dynamics, temperature and gas velocity fields substantially depend on tube diameter. Dependences of the flame velocity $S_{f,max}$ on the propagation distance for the tubes of different diameters are presented for the case with heat losses and adiabatic walls in Fig. 1a and b correspondingly.

According to the presented data flame front accelerates nearly linearly on the main part of the distance. At the starting 3–5 mm of the distance nonlinear velocity dependence is typical. Monotonous growth is characteristic for the case of adiabatic walls and non-monotonous—may take place in the case of non-adiabatic walls. Velocity and acceleration is considerably higher in the adiabatic case. In both cases the narrower tubes the higher flame velocity and acceleration. Flame velocity is close to the normal laminar flame speed (at the simulated distance) for the wider tubes ($d_0 \sim 1$ cm and higher) and may increase up to two orders of magnitude for narrower tubes at the distance of 2 cm from the closed end. Demonstrated dependence corresponds to the well known fact of detonation ignition length increase with tube diameter growth [1].

Flame velocity at the distance of 2 cm from the closed end as a function of the tube diameter is presented in Fig. 2. The curve corresponding to the adiabatic conditions lays higher than the curve calculated for the case of non-adiabatic walls. In the case of non-adiabatic walls the flame velocity grows monotonously with the tube diameter decrease until critical diameter reached. (For stoichiometric methane–air mixture at normal pressure and temperature calculations give $d_{cr} = 1.9$ mm or $d_{cr}/l_f = 6.3$.) Existence of the critical diameter is well known fact and connected with concurrence of heat release and heat losses of the flame. In the case of adiabatic walls flame continue to grow for $d < d_{cr}$ until diameter reaches some new critical value d_{cr1}, Fig. 2. Physical nature of the second critical diameter deserves analysis. Complex interaction of viscous tensions and heat release generated gas dynamics plays important role.

Simulation proves that flame velocity corresponds to the flame surface area (flame surface area law) with high accuracy, Fig. 3. For observation and analysis of the combustion gas dynamics the streamlines were drawn. Tangents to the streamlines correspond to the momentary velocity field. Note that for the non-steady case the streamlines do not correspond to the trajectories of particles. Nevertheless due to gas local quasi-steady movement in the system of coordinates moving with the front, streamlines effectively represent gas dynamics for the given combustion regime.

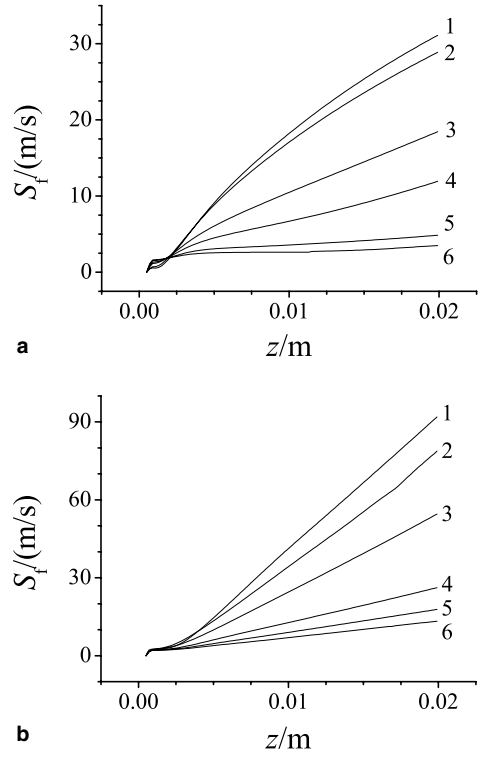

Fig. 1. Flame velocity $S_{f,max}$ as a function of the propagation distance for different diameters of the tube, (a) non-adiabatic walls: 1—$d_0 = 1.88$, 2—1.96, 3—2.48, 4—2.96, 5—3.96, 6—4.96 mm; (b) adiabatic walls: 1—$d_0 = 1$, 2—1.46, 3—1.96, 4—2.96, 5—3.96, 6—4.96 mm.

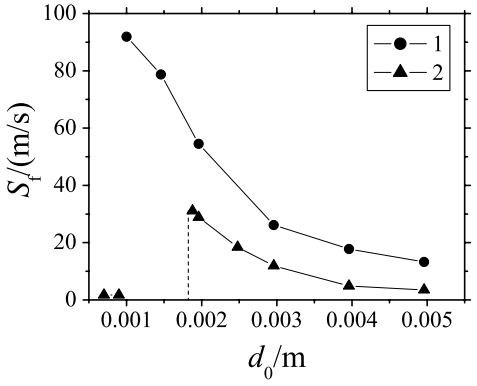

Fig. 2. Flame velocity $S_{f,max}$ at the distance of 3 cm from the closed end as a function of the tube diameter d_0. (●)—adiabatic walls; (▲)—non-adiabatic walls. Dashed line—thermal quenching limit.

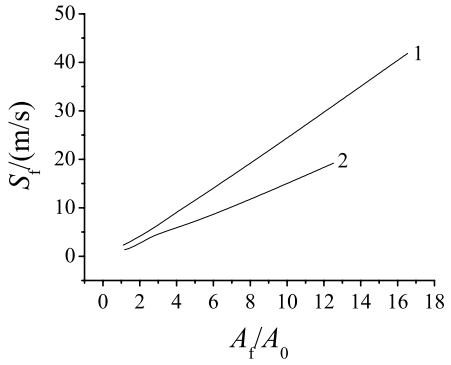

Fig. 3. Flame front velocity as function of dimensionless front square ($d_0 = 2.96$ mm): 1—for adiabatic walls; 2—for non-adiabatic walls.

Fig. 4 shows 2D temperature field and streamlines in the $d_0 = 2$ mm tube at the moment when flame reaches coordinate $z_{f,max} = 20.5$ mm.

Consequent shots of momentary streamlines give pictorial view of the process of the high velocity flame formation in the narrow tubes, as presented in Fig. 5 for the $d_0 = 2$ mm tubes. Based on the detailed numerical simulation one can mark out three stages of the flame evolution. First stage—formation of the front temperature and concentration profile. Perturbation of the front geometry is not strong. Acting as a semi-permeable piston, flame pushes combustible to the open end of tube. Formation of the parabolic gas dynamic profile starts. Front perturbation is mainly conditioned with gas drag at the walls. Streamlines (in the coordinates with the moving front) do not reveal peculiarities, Fig. 5a. At this first stage thermal quenching of the flame may take place in the case of heat losses prevail over heat generation ($d_0 < d_{cr}$) (Fig. 6).

The second stage is characterized by further velocity growth in conditions of considerable excess of the flame surface area over the initial flame surface area $A_f/A_0 \gg 1$. Flame acceleration remains approximately constant on the length of the tube ($\dot{m} \approx S_{f,max}$ and $\dot{m} \approx z_{f,max}$ consequently $S_{f,max} \sim z_{f,max}$). The beginning of this stage may be associated with front acceleration stabilization (constant inclination of the curves Fig. 1). Streamlines cross the flame front monotonously on the second stage.

As flame velocity grows a pulse to be transferred to the cold gas (and pressure before front) increases, specific displacement zone forms before the bow point of the flame front, Fig. 5b. Fresh gas flows around displacement zone. The width of the zone is close to the flame preheating width. Formation of displacement zone corresponds to emergence of the vortex as far as gas pushed ahead of the front meets fresh gas and turns back accepting pulse moment. Note that high velocity of flame is not sufficient for vortex formation. Vortex may appear if flame front has finger shape, because gas should have possibility to move to periphery of the

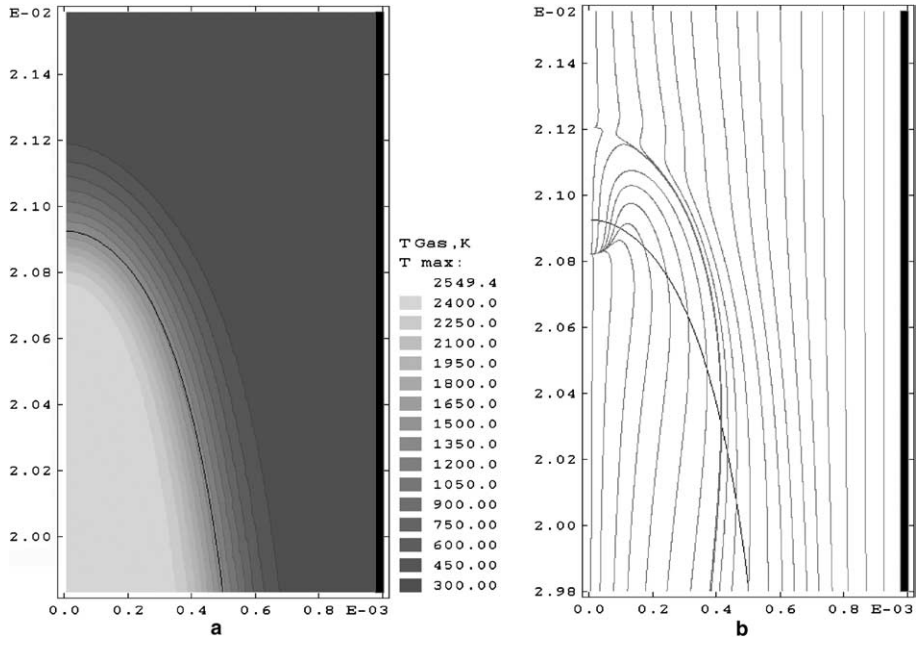

Fig. 4. Temperature field (a) and streamlines (b) in the system of coordinates moving with the front ($d_0 = 2$ mm). Black solid line—flame front.

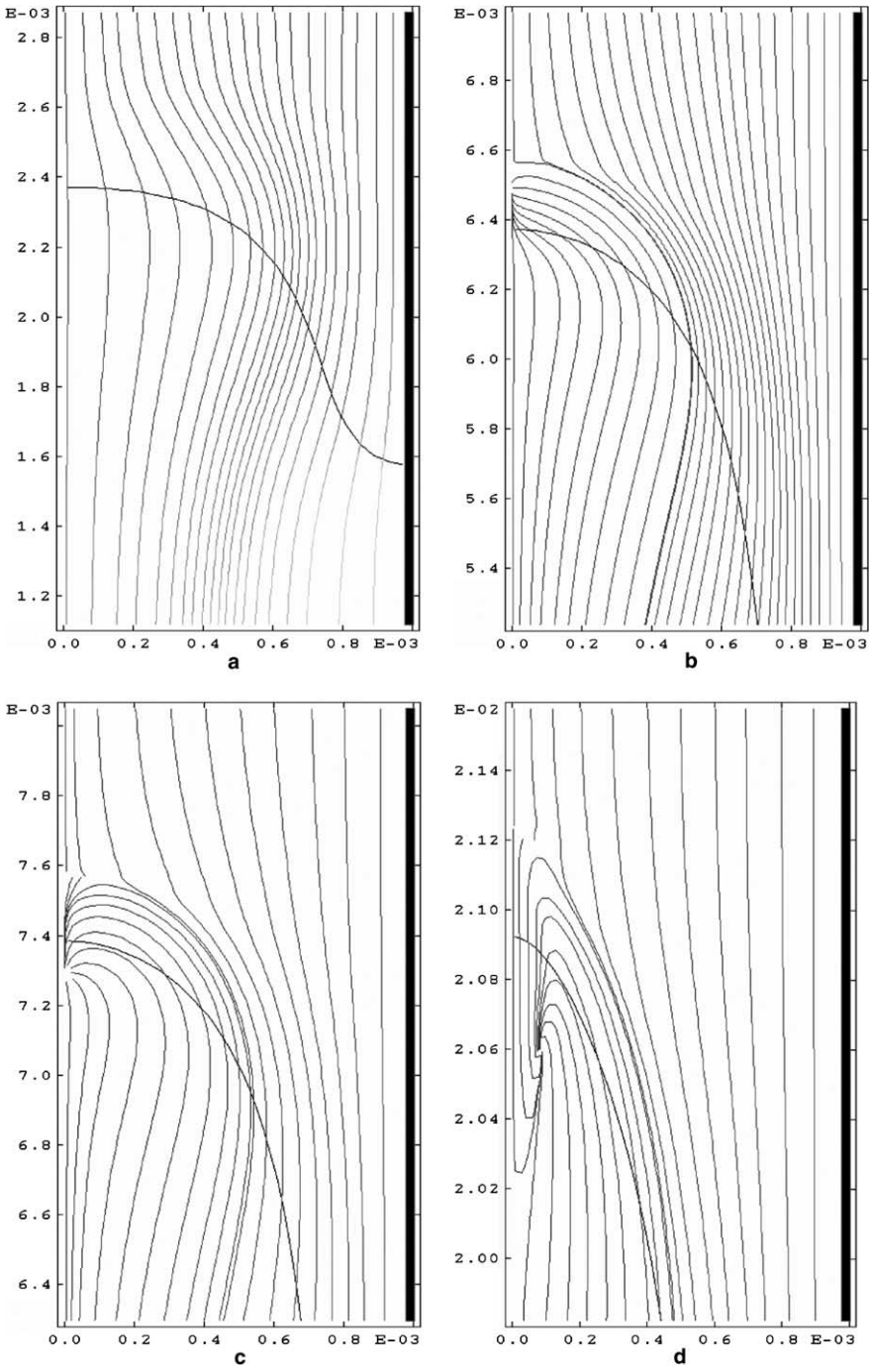

Fig. 5. Streamlines in the system of coordinates of flame front for tube ($d_0 = 2$ mm). Time instants: (a) $t = 8.1 \times 10^{-4}$, (b) 9×10^{-4}, (c) 1.3×10^{-3}, (d) 1.9×10^{-3} s.

channel. On practice, velocity increase and finger shape formation goes simultaneously.

Third stage is characterized by vortex formation in vicinity of the bow point of the combustion front and further acceleration of the flame. The vortex emerges in the displacement zone (Fig. 5b), then rapidly shifts under the front line (Fig. 5c) and increases its moment (Fig. 5d). Vortex induces additional perturbation of

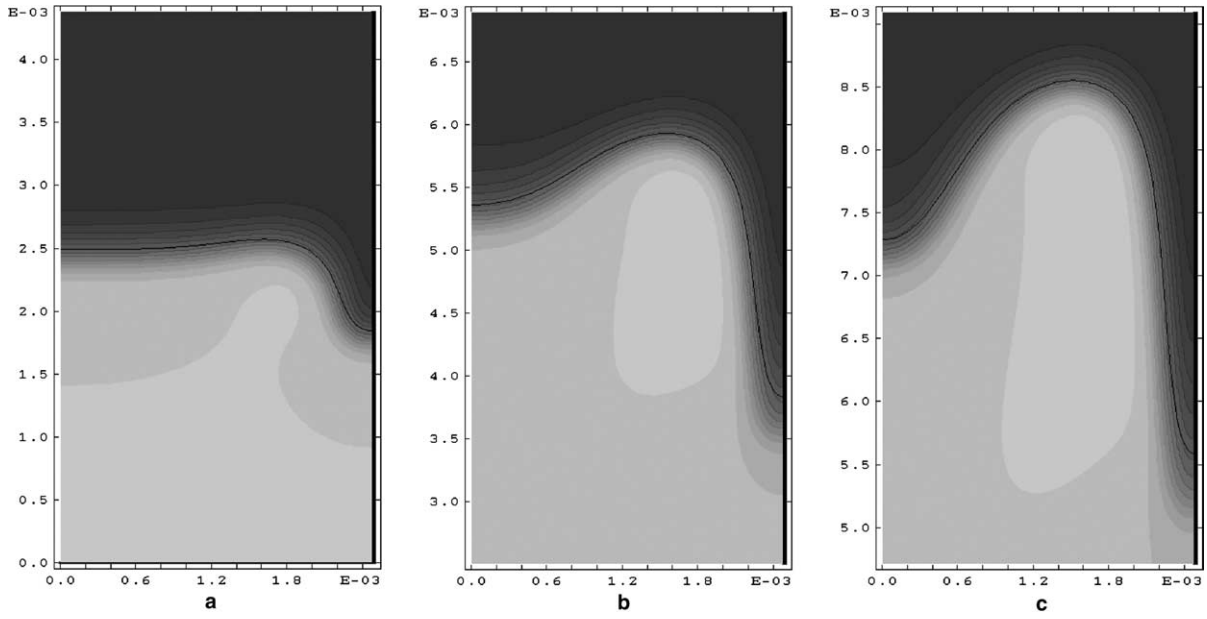

Fig. 6. Consequent shots of the temperature field for the combustion in the tube ($d_0 = 5$ mm). Time instants (a) $t = 1 \times 10^{-5}$, (b) 2×10^{-5}, (c) 2.5×10^{-5} s.

the gas flow field and may be considered a precursor of turbulence.

In the case of the "tulip" form geometry of the front (wider tubes) the same three stages of the accelerating flame evolution may be distinguished as in the case of the axial location of the leader ("mushroom" geometry of flame front). Particularly, when flame velocity reaches enough high value a vortex emerges in vicinity of the leader, Fig. 7. Note that propagation of flames in the form of adjacent to walls flame prominence and lagging central part, was observed experimentally [10].

In this work relatively short propagation paths were modeled and maximum flame velocity did not exceed 30 m/s in the case of non-adiabatic walls and 100 m/s in the case of the adiabatic walls. In the longer tubes higher velocities are reachable and one can expect emerging of more complicated flow and turbulization, although this is out of range of the paper.

In condition of adiabatic walls self sustained flame propagation is possible in narrow tube $d_0 \ll d_{cr}$. Combustion simulation at $d_0 < d_{cr}$ revealed a jump-like transition to a new regime (jump of the upper line at Fig. 2) at $d_0 = d_{cr1}$ (for the simulated system $d_{cr1} = 0.9$ mm). Physically formation of this regime is connected with the fact that strongly deformed flame structure cannot fit in thin tube (flame front width is equal or wider than the tube radius). Taking estimated value of the front width, in simulated case one obtains $d_{cr1}/l_f = 3$. New regime is characterized with relatively low flame propagation velocity, quasi-stationary front structure similar to "mushroom" shape and incomplete burn out of the fuel. Streamlines picture in vicinity of the flame front for this regime is presented in Fig. 8 in the system of coordinates of bound with moving front.

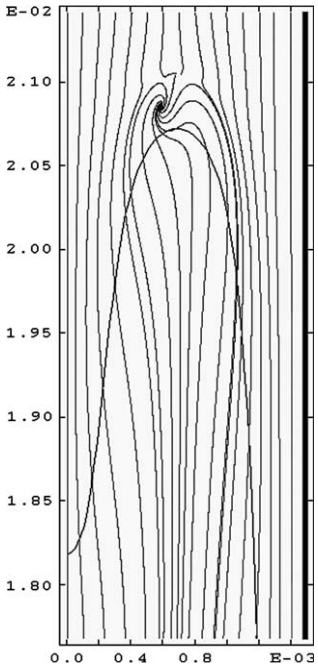

Fig. 7. Emerging of vortex in vicinity of the bow point of the flame front: $d_0 = 3$ mm, $t = 3.43 \times 10^{-3}$ s, $S_f = 26$ m/s.

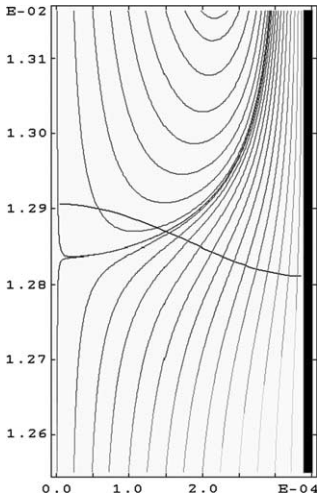

Fig. 8. Streamlines in vicinity of the flame front. Adiabatic walls, $d_0 = 0.7$ mm. Black solid line—combustion front. Flame propagation direction—from bottom to top.

One can observe a specific gas movement near the flame front. Although flame front has so-called "mushroom" geometry [6], gas dynamics resemble the movement of the particles at plough or bulldozer blade operation. Combustion front acts as semi-permeable bulldozer blade. It tears gas particles away from the wall and turns them to the direction of flame propagation. Following this analogy this regime can be named a *plough regime* of combustion. It is principal that combustion front turns fresh gas as well as combustion products and half products. As a result a mixture of fresh gas and combustion products is pulled before the front, energy balance of the flame front deteriorates and, combustion velocity becomes lower than normal flame propagation velocity in 1D semi-closed tube $[(\rho_0/\rho_b) - 1]S_l$, Fig. 9. Graph in Fig. 9 presents flame propagation velocity temporal evolution after ignition: non-steady perturbation and following relaxation to the quasi-steady constant value.

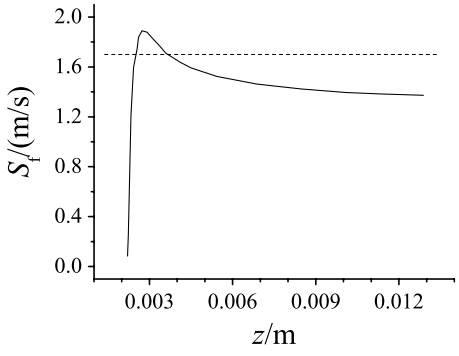

Fig. 9. Flame front velocity as a function of the distance from the tube's closed end. Adiabatic walls, $d_0 = 0.7$ mm. Dashed line—velocity corresponding to normal laminar flame propagation.

4. Conclusions

2D simulation of methane–air mixture combustion in narrow semi-closed tubes was performed for variable diameters of the tubes. It revealed gas dynamics of non-steady combustion and demonstrated formation of the vortex in vicinity of the front leading point—precursor of turbulence. Viscous deceleration of gas near the walls is the main factor of front perturbation. 2D test calculations with zero viscosity resulted in practically one dimensional solution for normal laminar flame.

Temperature field data are not informative for analysis of combustion gas dynamics. At the same time flow field in the system of coordinates bound with the front reveal complicated gas motions and let one observe vorticity emergence and evolution, Figs. 5 and 7.

New theoretically possible regime of combustion in thin tubes characterized with relatively small velocity and incomplete fuel burn out was found. This regime can hardly be realized for methane–air flames because of adiabatic walls condition requirement. The question of this regime realization in other systems, for example, liquid monofuels deserves investigation.

Acknowledgement

The work was partially supported by the INTAS grant # 03-51-4736.

References

[1] Ya.B. Zeldovich, G.I. Barenblat, A.G. Librovich, G.I. Makhviladze, Mathematical Theory of Combustion and Explosion, Bureau Consultants, New York, 1980.
[2] F.A. Williams, Combustion Theory, second ed., The Benjamin Cummings Publishing Co., Menlo Park, CA, 1985.
[3] A.I. Rozlovski, Fundamentals of Explosion Safety at Gases and Vapors Operation, Khimia Publ., Moscow, 1980 (in Russian).
[4] O.Yu. Travnikov, V.V. Bychkov, M.A. Liberman, Numerical studies of flames in wide tubes: stability limits of curved stationary flames, Phys. Rev. E 61 (2000) 468–474.
[5] R.C. Aldredge, B. Zuo, Flame acceleration associated with the Darrieus–Landau instability, Combust. Flame 127 (2001) 2091–2101.
[6] J. Jarosinski, R.A. Strehlow, A. Azarbarzin, The mechanism of lean limit extinguishment of an upward and downward propagating flame in a standard flammability tube, in: 19th Symp. (Int.) on Combustion, The Combustion Institute, Pittsburgh, 1982, p. 1549.

[7] D. Dunn-Rankin, P.K. Barr, R.F. Sawyer, Numerical and experimental study of "tulip" flame formation in a closed vessel, in: 21st Symp. (Int.) on Combustion, The Combustion Institute, Pittsburgh, 1986, p. 1291.
[8] S.T. Lee, J.S. Tien, A numerical analysis of flame flashback in a premixed laminar system, Combust. Flame 48 (1982) 273–285.
[9] K.I. Schelkin, On theory of detonation development in gases, DAN USSR 23 (7) (1939) 636–640 (in Russian).
[10] R.I. Soloukhin, Shock Waves and Detonation in Gases, Monoboo Corp., Baltimore, 1966.
[11] A.K. Oppenheim, Ann. Rev. Fluid Mech. 5 (1973) 31–58.
[12] J. Daou, M. Matalon, Flame propagation in Poiseuille flow under adiabatic conditions, Combust. Flame 124 (2001) 337–349.
[13] J. Daou, M. Matalon, Influence of conductive heat losses on the propagation of premixed flames in channels, Combust. Flame 128 (2002) 321–339.
[14] I. Brailovski, G.I. Sivashinski, Momentum loss as a mechanism for deflagration to detonation transition, Combust. Theory Modell. 2 (1998) 429–447.
[15] L. Kagan, G.I. Sivashinski, The transition from deflagration to detonation in thin channels, Combust. Flame 134 (4) (2003) 389–397.
[16] D. Ott, A mechanism for flame acceleration in narrow tubes, AIAA J. 41 (7) (2003) 1391–1396.
[17] R.J. Kee, F.M. Rupley, J.A. Miller, M.E. Coltrin, J.F. Grcar, E. Meeks, H.K. Moffat, A.E. Lutz, G. Dixon-Lewis, M.D. Smooke, J. Warnatz, G.H. Evans, R.S. Larson, R.E. Mitchell, L.R. Petzold, W.C. Reynolds, M. Caracotsios, W.E. Stewart, P. Glarborg, C. Wang, O. Adigun, W.G. Houf, C.P. Chou, S.F. Miller, P. Ho, D.J. Young, CHEMKIN Release 4.0, Reaction Design, Inc., San Diego, CA, 2004.
[18] L. Hackert, J.L. Ellzey, O.A. Ezekoye, Effects of thermal boundary conditions on flame shape and quenching in ducts, Combust. Flame 112 (1998) 73–84.
[19] K. Hanamura, R. Echigo, S.A. Zhdanok, Superadiabatic combustion in a porous medium, Int. J. Heat Mass Transfer 36 (13) (1993) 3201–3209.
[20] K.V. Dobrego, I.M. Kozlov, N.N. Gnezdilov, V.V. Vasiliev 2DBurner—software package for gas filtration combustion systems simulation and gas no-steady flames simulation, Preprint no. 1, Heat and Mass Transfer Institute, Minsk, 2004.
[21] I.M. Kozlov, A.Ye. Suvorov, V.I. Tyukaev, A numerical study of free convection in a strongly inhomogeneous gas medium, Int. J. Heat Mass Transfer 38 (1995) 2689–2695.